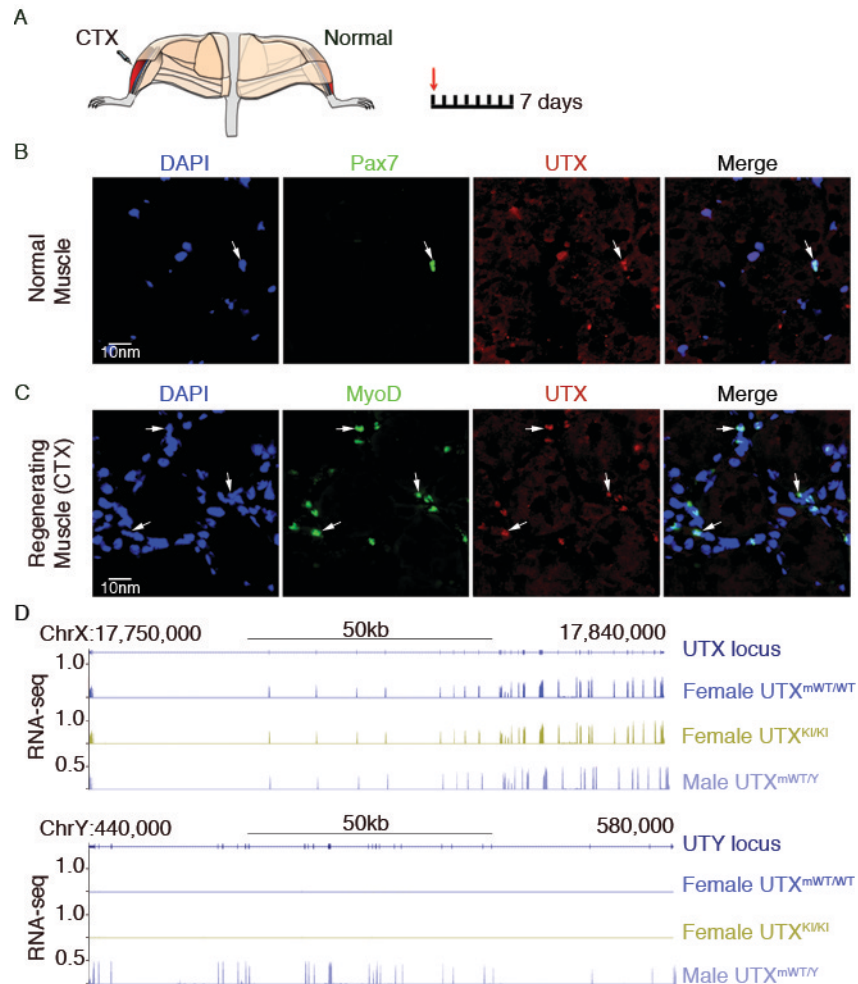


## **UTX/KDM6A demethylase activity is required for satellite cell-mediated muscle regeneration**

Hervé Faralli<sup>1,2</sup>, Chaochen Wang<sup>3</sup>, Kiran Nakka<sup>1,2</sup>, Soji Sebastian<sup>1,¶</sup>, Aissa Benyoucef<sup>1,2</sup>, Lenan Zhuang<sup>3</sup>, Alphonse Chu<sup>1,2</sup>, Carmen Palii<sup>1,2</sup>, Chengyu Liu<sup>4</sup>, Brendan Camellato<sup>1,5</sup>, Marjorie Brand<sup>1,2,5</sup>, Kai Ge<sup>3</sup> and F. Jeffrey Dilworth<sup>1,2,5</sup>

<sup>1</sup>Sprott Center for Stem Cell Research, Ottawa Hospital Research Institute, Ottawa, ON, Canada, K1H 8L6; <sup>2</sup>Ottawa Institute of Systems Biology, University of Ottawa, ON, Canada, K1H 8L6; <sup>3</sup>National Institute of Diabetes & Digestive & Kidney Diseases, National Institutes of Health, Bethesda, MD, USA 20892; <sup>4</sup>Transgenic Core, Center for Molecular Medicine, National Heart, Lung, and Blood Institute, National Institutes of Health, Bethesda, MD, USA 20892; <sup>5</sup>Department of Cellular and Molecular Medicine, University of Ottawa, ON, Canada, K1H 8L6.

## **SUPPLEMENTAL INFORMATION**



**Figure S1: UTX and UTY expression in adult satellite cells.** **(A)** Illustration of the experimental procedure; time of cardiotoxin (CTX) injection is represented by a red arrow. **(B, C)** Confocal optical views of transverse sections through the tibialis anterior skeletal muscle of UTX<sup>mWT</sup> mice (magnification 60X). **(B)** IF on non-injured muscle (Normal Muscle) to visualize DAPI (blue), Pax7 (green) and UTX (red) positive cell populations. **(C)** IF on regenerating muscle to visualize DAPI (blue), MyoD (green) and UTX (red) positive cell populations. **(D)** RNA-Seq tracks taken from analysis of differentiating primary myoblasts from female UTX<sup>mWT/WT</sup> or male UTX<sup>mWT/Y</sup> mice. This shows that myoblasts from males express ~50% of the number of UTX (X chromosome) transcripts compared to those isolated from females. This decrease in UTX expression in males is compensated by an equal number of UTY (Y chromosome) transcripts.

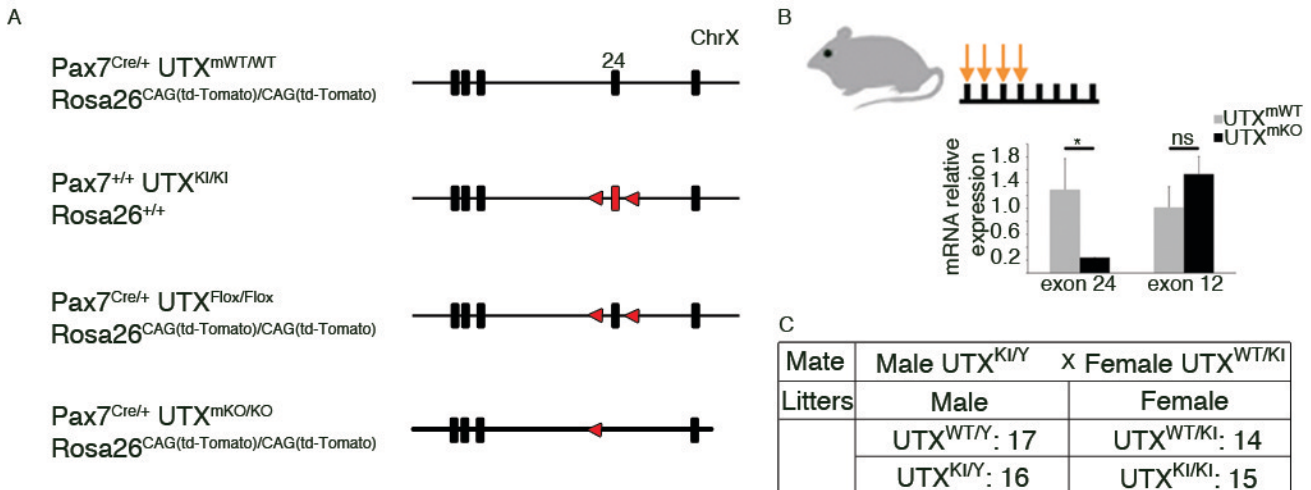


**Figure S2: Generation of the UTX transgenic mice. (A)** Schematic representation of the UTX locus in our various mouse genotypes. The unaltered UTX allele has a genotype of Pax7<sup>Cre/+</sup> UTX<sup>mWT/WT</sup> Rosa26<sup>CAG(td-Tomato)/CAG(td-Tomato)</sup> (referred to as UTX<sup>mWT</sup>). The mouse Pax7<sup>+/+</sup>;UTX<sup>KI/KI</sup>;Rosa26<sup>+/+</sup> carries the enzyme-dead knock-in allele (referred to as UTX<sup>KI</sup>). The UTX<sup>KI</sup> allele possesses the H1146A and E1148A point mutations in exon 24 (red box). The Pax7<sup>Cre/+</sup>;UTX<sup>Flox/Flox</sup>;Rosa26<sup>CAG(td-Tomato)/CAG(td-Tomato)</sup> (referred to as UTX<sup>Flox</sup> conditional allele) contains a pair of Flox sites (red triangle) flanking exon 24. The Pax7<sup>Cre/+</sup>;UTX<sup>mKO/mKO</sup>;Rosa26<sup>CAG(td-Tomato)/CAG(td-Tomato)</sup> (referred to as UTX<sup>mKO</sup>) is generated by deletion of exon 24 from the Floxed allele by tamoxifen-induced Cre recombination. The Pax7<sup>Cre/+</sup>;UTX<sup>Flox/KI</sup>;Rosa26<sup>CAG(td-Tomato)/+</sup> (referred to as UTX<sup>mWT/KI</sup>) carries the enzyme-dead knock-in on one allele and the UTX<sup>Flox</sup> conditional allele contains two Flox sites (red triangle) flanking exon 24. The Pax7<sup>Cre/+</sup>;UTX<sup>mKO/KI</sup>;Rosa26<sup>CAG(td-Tomato)/+</sup> (referred to as UTX<sup>mKO/KI</sup>) is generated by deletion of exon 24 from the one Floxed allele by Cre-recombinase. **(B)** After four daily Tamoxifen injections (orange Arrow) and 3 days of recovery, primary myoblast were isolated from UTX<sup>mWT</sup> and UTX<sup>mKO</sup> mice. UTX expression levels after Cre-mediated excision was determined by quantitative RT-PCR analysis (normalized to GAPDH) by using two different pair of primers: one targeting exon 12 and the other exon 24. Values represent average expression relative to GAPDH  $\pm$  standard deviation. Statistical analysis was performed using an unpaired t test where \* indicates  $p < 0.05$  or while ns. indicates not significant, n = 3. **(C)** UTX<sup>KI</sup> mice are born at expected the Mendelian ratio. Table of UTX<sup>KI</sup> pup genotyping from 10 litters at weaning age of post-natal day 21 based on mating of male UTX<sup>KI/Y</sup> with female UTX<sup>WT/KI</sup> mice.

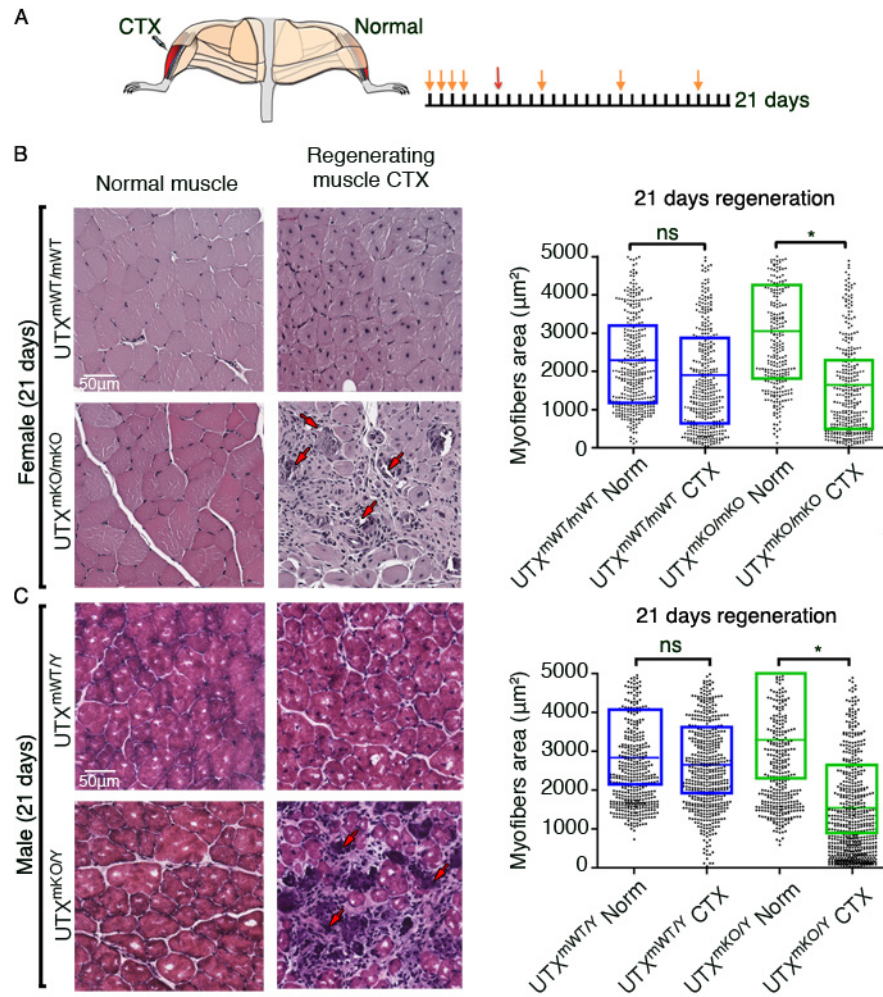


**Figure S3: Muscle regeneration continues to be impaired at late stages of regeneration in UTX<sup>mKO</sup>.** (A) Schematic illustration of the experimental procedure; tamoxifen injections are represented by orange arrows and cardiotoxin injection by a red arrow. (B and C) Histological analysis of TA muscle was performed using Hematoxylin/Eosin staining of muscle that had not been injured (normal muscle) or had been allowed to regenerate for 21 days after cardiotoxin injury (regenerating muscle). Necrotic tissue and infiltrating immune cells are indicated by red arrows. Muscle sections from (B) female UTX<sup>mKO/mKO</sup> and (C) male UTX<sup>mKO/Y</sup> mice were visualized under 20X magnification and represent a total area of 90,000  $\mu\text{m}^2$ . Myofiber calibers within the TA muscle were calculated and plotted for each condition ( $n > 1000$  total fibers per condition). Each dot represents the area of a single myofiber, the horizontal bar correspond to the mean within the 95% confidence interval (box). Statistical significance was determined using an ANOVA test where \* indicates  $p < 0.05$ . Measurements have been performed on a minimum of 3 mice taken from 3 independent experiments.

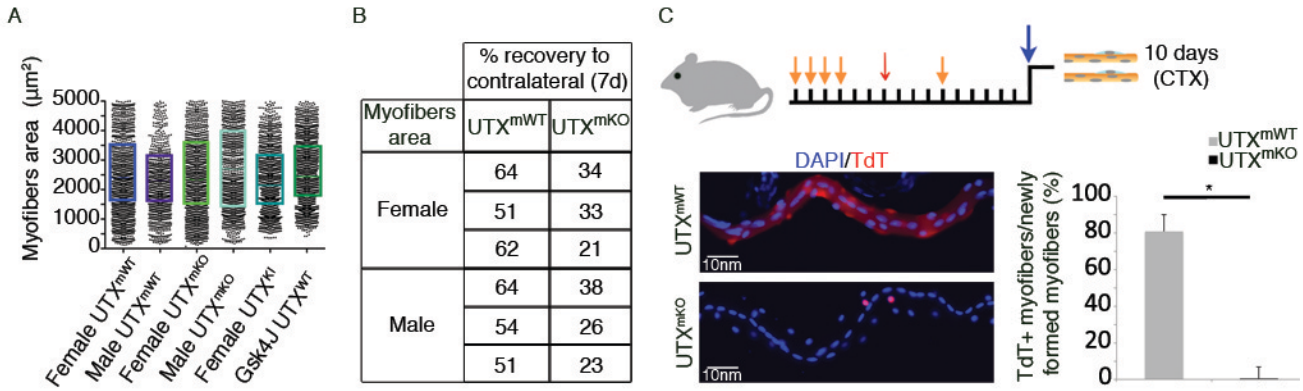


**Figure S4:** (A) Myofiber size in healthy TA muscle is not significantly affected by loss of UTX. The average caliber size of uninjured TA muscles from the various UTX mouse genotypes has been calculated using 9 mice taken from 3 independent experiments. (B) Myofiber repair efficiency is compromised in the absence of UTX. The percentage of recovery was calculated by determining the mean cross-sectional area of regenerating muscle fibers at 7 days after cardiotoxin treatment as a percentage of the mean cross sectional area of the control TA muscle that remained uninjured. (C) Newly formed myofibers in the  $\text{UTX}^{\text{mKO}}$  mouse are derived from SCs that escape Cre-mediated recombination. Illustration of the experimental procedure where tamoxifen injections are represented by orange arrows and cardiotoxin injection by a red arrow, and the time of myofiber isolation from the injured EDL is represented by the blue arrow. Newly formed myofibers (identified by centrally located nuclei) from female  $\text{UTX}^{\text{mKO/KO}}$  and  $\text{UTX}^{\text{mWT/WT}}$  mice were visualized by fluorescence microscopy (20X magnification). TdT+ newly formed fibers were quantitated and are represented as a percentage of the total numbers of newly formed fibers  $\pm$  standard deviation. Statistical significance was determined using an unpaired t-test where \* indicates  $p < 0.05$ . Count have been performed on  $> 100$  myofibers per groups in three independent experiments.

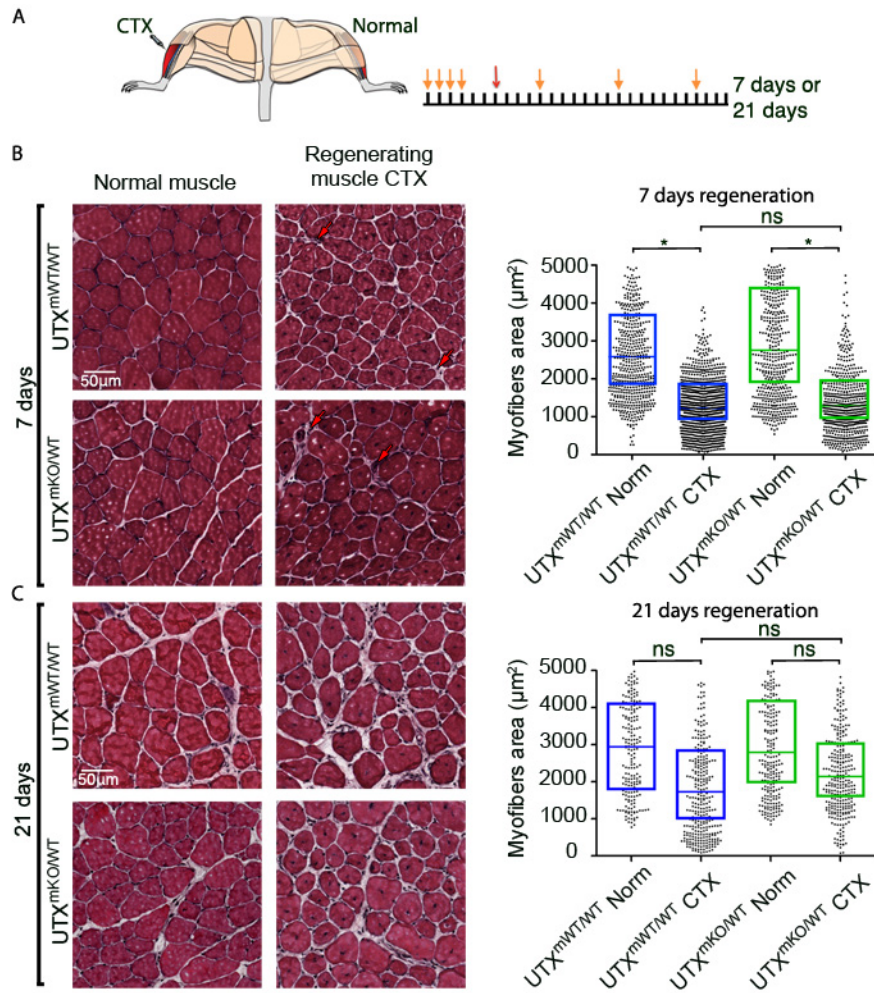


**Figure S5: A single allele of UTX is sufficient to ensure efficient muscle regeneration.** (A) Schematic illustration of the experimental procedure; tamoxifen injection is represented by an orange arrow and cardiotoxin injection by a red arrow. (B, C) Histological analysis of TA muscle of wild-type (UTX<sup>mWT/WT</sup>) or heterozygous UTX mutant (UTX<sup>mKO/WT</sup>) mice was performed using Hematoxylin/Eosin staining of muscle that had not been injured (normal muscle) or had been allowed to regenerate for either (B) 7, or (C) 21 days after cardiotoxin injury (regenerating muscle). Necrotic tissues and the infiltrating interstitial cells are indicated by red arrows. Muscle sections were visualized under 20X magnification and represent a total area of 90,000  $\mu\text{m}^2$ . Myofiber calibers within the TA muscle of UTX<sup>mWT/WT</sup> and UTX<sup>mKO/WT</sup> mice were calculated and plotted for each condition ( $n > 1000$  total fibers per condition). Each dot represents the area of a single myofiber, the horizontal bar correspond to the mean within the 95% confidence interval (box). Statistical significance was determined using an ANOVA test where \* indicates  $p < 0.05$ . Measurements have been performed on a minimum of 3 mice taken from 3 independent experiments.

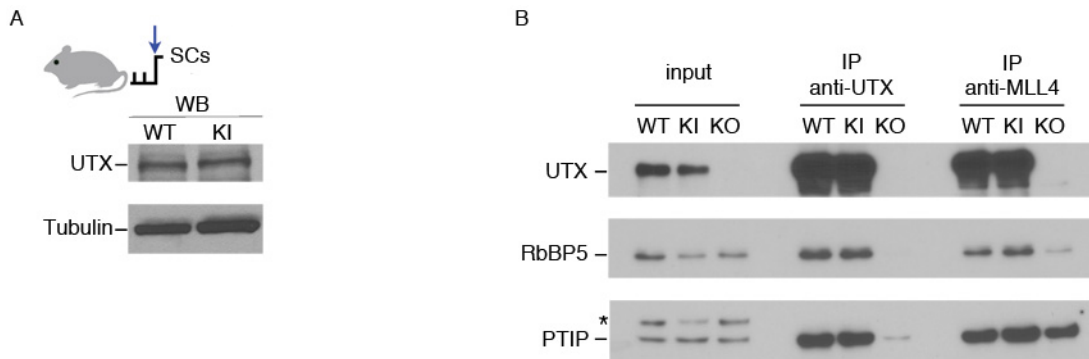


**Figure S6: The demethylase dead UTX protein is stable and can complex with Trr-like complex in cells.**  
**(A)** Whole cell protein extracts prepared from  $UTX^{mWT}$  and  $UTX^{KI/KI}$  myoblasts were analyzed by Western blot for the expression of UTX protein. Tubulin is provided as a loading control. **(B)** MLL4 complex is intact in  $UTX^{KI}$  cells. Immunoprecipitation was performed using anti-UTX and anti-MLL4 antibodies in nuclear extracts of wild-type(WT), knockin(KI) and knockout(KO) embryonic stem cells. Western blot was performed using the antibodies indicated. A non-specific band recognized by the PTIP antibody is labeled with asterisk.

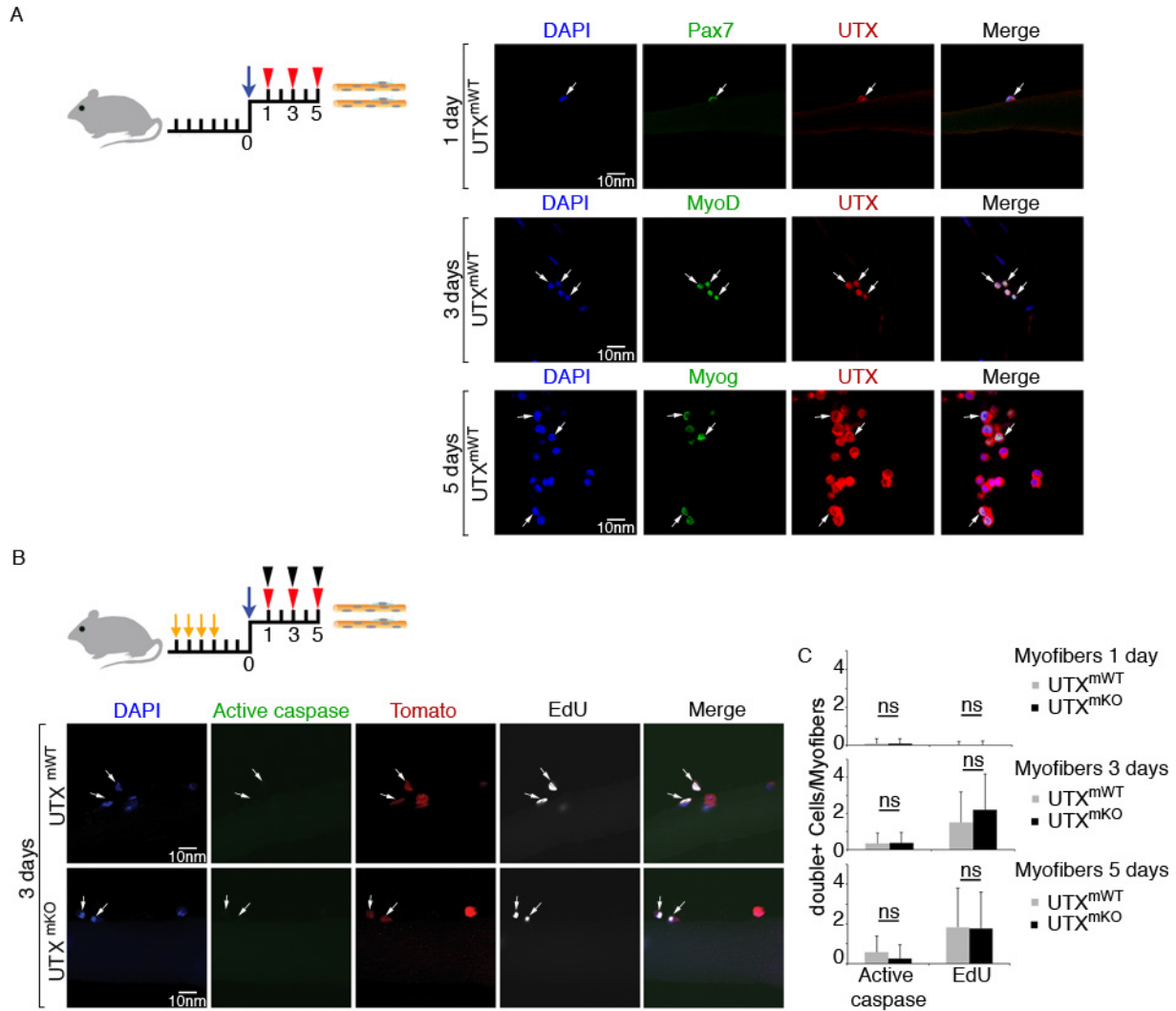


**Figure S7: The absence of UTX does not affect the ability of myogenic progenitor cells to proliferate.**

**(A)** Schematic illustration of the experimental procedure where myofiber isolation is represented by the blue arrow. Freshly isolated myofibers from extensor digitorum longus (EDL) muscles of UTX<sup>mWT</sup> mice were cultured in growth medium for 1, 3, or 5 days. At specified time points, myofibers were stained and analyzed for colocalization of UTX (red) with either Pax7, MyoD, or Myog (green as indicated) amongst the DAPI (blue) stained nuclei (confocal optical view original magnification 60X).

**(B)** Schematic illustration of the experimental procedure, with tamoxifen injection represented by orange arrow, myofibers isolation by blue arrow. Myofibers freshly isolated from EDL muscles of UTX<sup>mWT</sup>, or UTX<sup>mKO</sup> mice were cultured in growth medium for 1, 3, or 5 days. Prior to myofiber fixation, a 2h pulse of EdU was performed to mark dividing cells (black arrowheads). These same myofibers were then immunostained for active caspase at different time points (red arrowheads). Tomato<sup>+</sup> cells are indicated by white arrows (confocal optical view original magnification 60X). Hoescht (blue), active caspase (green), Tomato (red) and EdU (white).

**(C)** The number of Tomato<sup>+</sup> cells that proliferate (EdU<sup>+</sup>) or undergo to apoptosis (active caspase<sup>+</sup>) per myofibers was evaluated and represented as an average number of positive cells per field ± standard deviation. Statistical significance was determined using an unpaired t-test where n.s. indicates not significant.

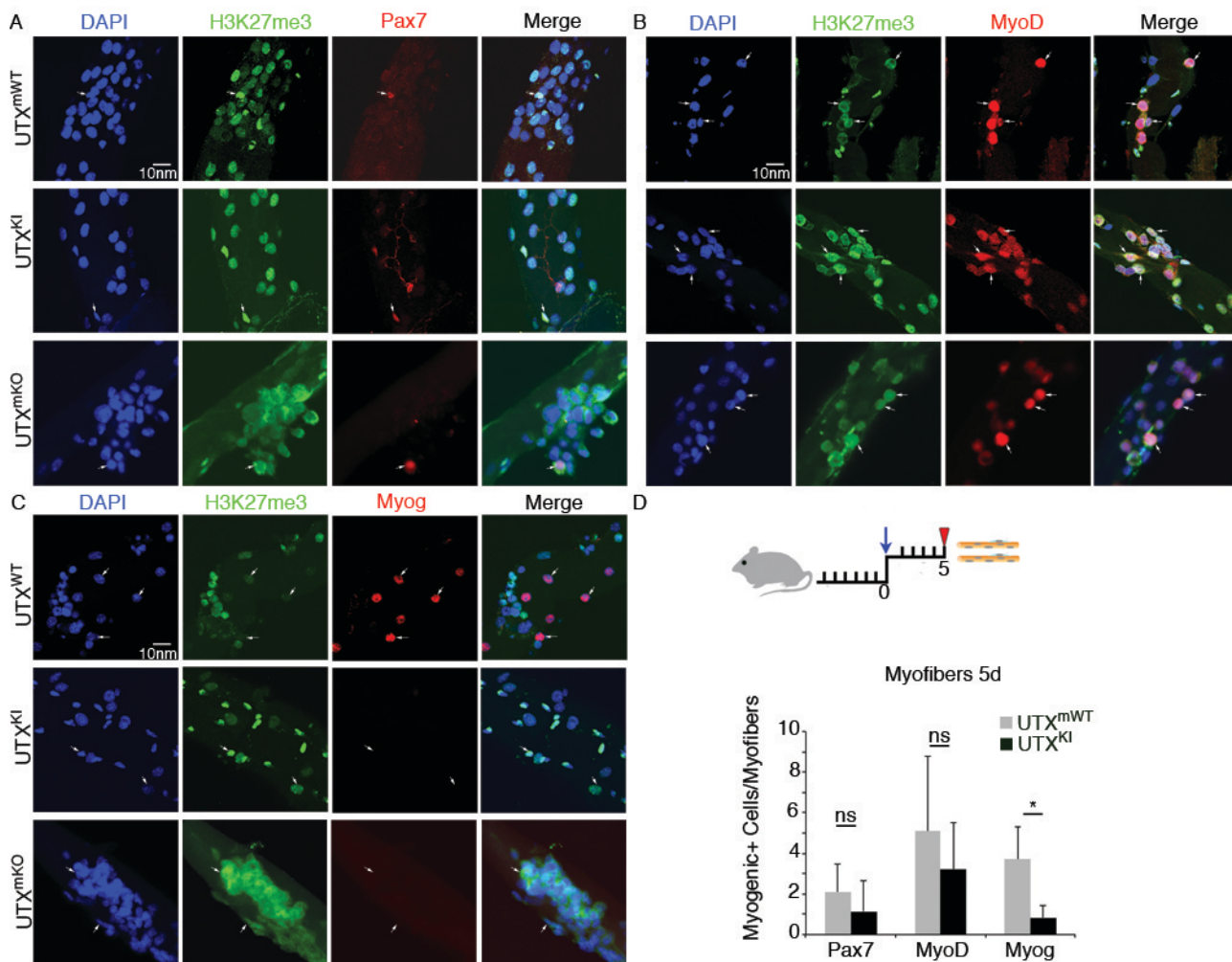


**Figure S8: Muscle progenitor cells from the UTX<sup>KI</sup> mice are unable to differentiate *ex vivo*.** (A-C) Extensor digitorum longus (EDL) myofibers were isolated from UTX<sup>WT</sup> or UTX<sup>KI</sup> or UTX<sup>mKO</sup> mice. Myofibers cultured for 5 days *ex vivo* were stained and analyzed for colocalization of H3K27me3 (green) with Pax7 (A), MyoD (B), or Myog (C) (red as indicated) amongst the DAPI (blue) stained nuclei (confocal optical view original magnification 60X). (D) Schematic illustration of the experimental procedure, myofibers isolation is represented by blue arrow and IF by red arrowhead. The number of cells expressing specific each myogenic markers was quantitated and is represented as an average number of myogenic transcription factor positive cells per fiber  $\pm$  standard deviation. Statistical significance was determined using an unpaired t-test where \* indicates  $p < 0.05$  or while n.s. indicates not significant. Count have been performed on  $> 100$  myofibers per groups in three independent experiments.

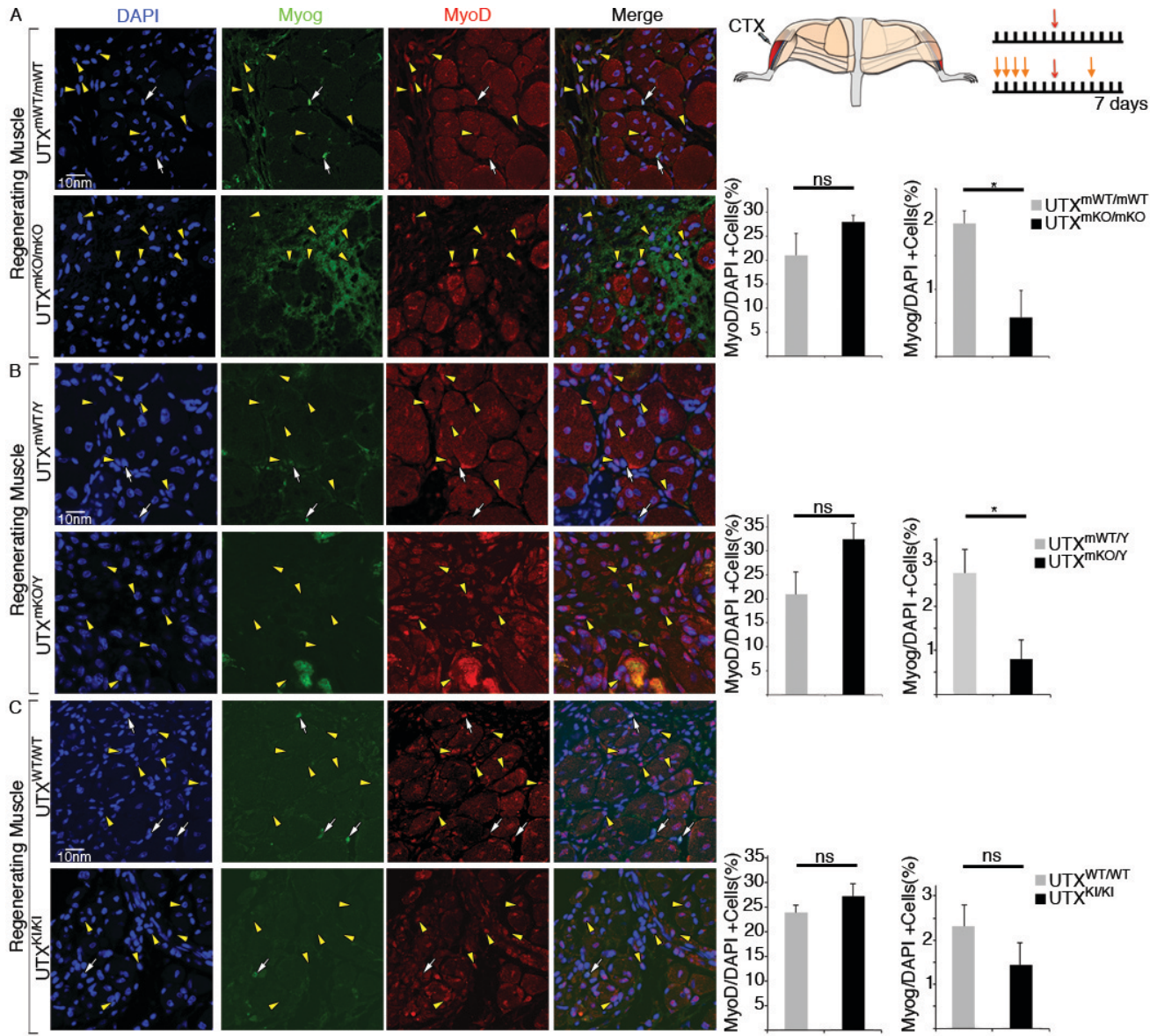


**Figure S9: Myog expression is impaired *in vivo* during the muscle regeneration of the UTX<sup>mKO</sup> and UTX<sup>KI</sup> mice.** The experimental procedure is schematic illustrated where tamoxifen injection is represented by an orange arrow and cardiotoxin injection by a red arrow. Confocal optical views of transverse sections through (A) female UTX<sup>mWT</sup> and UTX<sup>mKO</sup>, (B) male UTX<sup>mWT</sup> and UTX<sup>mKO</sup>, and (C) female UTX<sup>mWT</sup> and UTX<sup>KI/KI</sup> TA muscles (original magnification 60X). IF staining for MyoD/Myog have been performed where DAPI (blue) Myog (green) and MyoD (red). MyoD<sup>+</sup> cells are identified by yellow arrowhead and Myog<sup>+</sup> cells by white arrows. MyoD<sup>+</sup> and Myog<sup>+</sup> cells were enumerated as a percentage of the total number of nuclei. Values presented in the graph are the average number of MyoD<sup>+</sup> or Myog<sup>+</sup> cells observed in 120 fields of view observed from 3 mice from 3 independent experiments. Statistical significance was determined using an unpaired t-test where \* indicates  $p < 0.05$  or while n.s. indicates not significant.

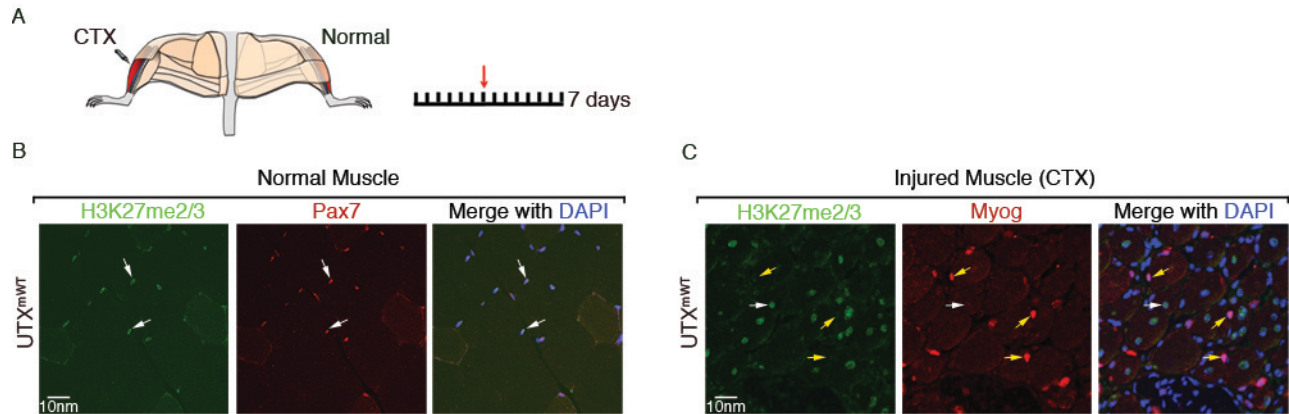


**Figure S10: Muscle progenitor cells from the UTX<sup>KI</sup> mice are unable to differentiate *in vivo*.** (A) Schematic illustration of the experimental procedure where tamoxifen injection is represented by an orange arrow and cardiotoxin injection by a red arrow. (B-C) Confocal optical views of transverse sections through the TA muscle derived from UTX<sup>mWT</sup> (original magnification 60X). (B) IF staining for H3K27me2/3 and Pax7 have been performed where DAPI (blue) H3K27me2/3 (green) and Pax7 (red). Pax7<sup>+</sup> cells are identified by white arrow. (C) IF staining for H3K27me2/3 and Myog have been performed where DAPI (blue) H3K27me2/3 (green) and Myog (red). Myog<sup>+</sup> cells are identified by yellow arrowhead and some H3K27me2/3<sup>+</sup> cells by white arrows.

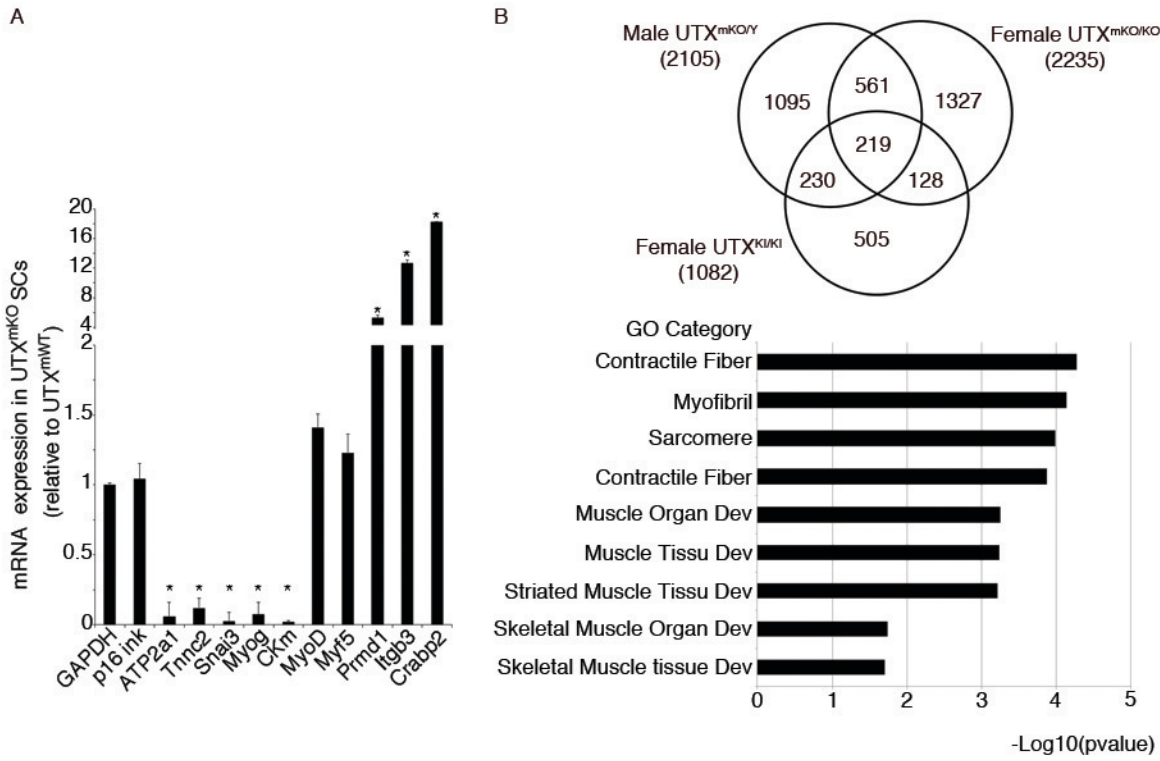


**Figure S11: UTX regulates the muscle gene expression program.** (A) Independent isolates of RNA were used in RT-qPCR assays to validate a subset of up- and down-regulated genes identified in the RNA-Seq experiments. Relative gene expression is corrected for the internal control GAPDH and is presented as the average expression in  $UTX^{mKO/TdT}$  cells compared to  $UTX^{mWT/TdT}$  cells  $\pm$  standard deviation. Values are presented as the average enrichment as a percentage of input  $\pm$  standard deviation. Statistical analysis was performed using an unpaired t test where \* indicates  $p < 0.05$  or while n.s. indicates not significant,  $n = 3$ . (B) RNA-Seq analysis was performed to identify genes whose expression is modified in differentiation myoblasts from  $UTX^{mKO/TdT}$ ,  $UTX^{K1/K1}$ , and  $UTX^{mWT/TdT}$  mice. The overlap of 219 genes that are downregulated in male, female  $UTX^{mKO/TdT}$  and female  $UTX^{K1/K1}$  mice is represented by a Venn diagram. Gene Ontology (GO) analysis of the 219 genes down-regulated in myoblasts from male, female  $UTX^{mKO/TdT}$  and female  $UTX^{K1/K1}$  shows highly significant enrichment of genes involved in muscle development and function.

**Supplemental Table 2 – Primers Used in the study**

<b>Genotyping Primers</b>	
UTX gn-1	5'-AACAAAAACCCAGGCTTATTCAC-3'
UTX gn-2	5'-AGTTTCAGGATACCTTACTATAAG-3'
UTX-24F	5'-CATCAAGAAAATAACAACCTCTGTCAGT-3'
Up-IntCre	5'-TTTGCCTGCATTACCGGTCGATGC-3'
intCre-rev	5'-TCCATGAGTGAACGAACCTGGTCG-3'
ROSA26 Tdt WT Forward	5'-AAGGGAGCTGCAGTGGAGTA-3'
ROSA26 Tdt WT Reverse	5'-CCGAAAATCTGTGGGAAGTC -3'
ROSA26 Tdt MUT Forward	5'-GGCATTAAAGCAGCGTATCC-3'
ROSA26 Tdt MUT Reverse	5'-CTGTTCCCTGTACGGCATGG-3'
<b>Expression Primers</b>	
F: Myog	5'-CATCCAGTACATTGAGCGCCTACA-3'
R: Myog	5'-AGCAAATGATCTCCTGGGTTGGGA-3'
F: MyoD	5'-TGAGCAAAGTGAATGAGGCCTTCG-3'
R: MyoD	5'-TGCAGACCTCGATGTAGCGGAT-3'
F: Myf5	5'-TGAGGGAACAGGTGGAGAAC-3'
R: Myf5	5'-AGCTGGACACGGAGCTTTA-3'
F: Desmin	5'-ATGAGACCATCGCGGCTAAGAAC-3'
R: Desmin	5'-ATTGGCTGCCTGAGTCAAGTCTGA-3'
F: MyHC	5'-ACCTTGCCAAGAAGAAGGACTCCA-3'
R: MyHC	5'-TGGATGCGGATGAACTTGCCAAAG-3'
F: DDX5	5'-TTCTGATTGCTACCGATGTGGCCT-3'
R: DDX5	5'-TGGTACTGCGAGCAGTTCTTCAA-3'
F: GAPDH	5'-TCAAGAAGGTGGTGAAGCAGG-3'
R: GAPDH	5'-ACCAGGAAATGAGCTTGACAAA-3'
F: UTX exon24	5'-GGTGACTGTGAATGGTTGTT-3'
R: UTX exon 24	5'-AGTAAGCTGTCCTTGAGATACTG-3'
F: UTX	5'-TACCTCTGGACTTGCAGCACGAATTA-3'
R: UTX	5'-TTGCCACCACTCCAATTATCAGAA-3'
F: ATP2a1	5'-CAATCAGTCGGCTCTATG-3'
R: ATP2a1	5'-TTGTTCTCCATGTAGCCGTG-3'
F: TnnC2	5'-AGATGAAAGAGGATGCGAAGG-3'
R: TnnC2	5'-AGAAGCCCGGAAAATCTCAG-3'
F: Snai3	5'-TGCCCCTCAAGATGCATATCC-3'
R: Snai3	5'-GCAGTGAGAACAGGTATAGGG-3'
F: Prdm1	5'-ATTAAGCCTATCCCTGCCAAC-3'
R: Prdm1	5'-CTACTGTATTGCTTGGGTTGC-3'
F: Itgb3	5'-TCGTCAGCCTTACCAAGAATT-3'
R: Itgb3	5'-CGTACTTCCAGCTCCACTTAG-3'
F: Crabp2	5'-AGCGTCCAGTGTCTAGTTG-3'
R: Crabp2	5'-TCCAGTTGCCAGAAAAGTTAGG-3'
<b>ChIP Primers</b>	
F: Promoter Myog	5'-TCACATGTAATCCACTGGAAACG-3'

R: Promoter Myog	5'-CCTGAGCCCCCTCTAAG-3'
F: Promoter CKm	5'-TAGTCACACCCTGTAGGCTCCTCTAT-3'
R: Promoter CKm	5'-ATTCTCTCAGTCCCTACCTGGCT
F: Promoter Tnnc2	5'-TGAAAGTGGAGAGCAGAGAAA-3'
R: Promoter Tnnc2	5'-TGATTAGCGACTGTCCATGA-3'
F: Gene Desert chr15	5'-TCCTCCCCATCTGTGTCATC-3'
R: Gene Desert chr15	5'-GGATCCATCACCATCAATAACC-3'